






RESEARCH ARTICLE | AUGUST 29 2023

# The effect of the cell tilting on the temperature oscillation in turbulent Rayleigh–Bénard convection

Xin Chen (陈鑫)   ; Ao Xu (徐翱)  ; Ke-Qing Xia (夏克青)  ; Heng-Dong Xi (郗恒东)  



*Physics of Fluids* 35, 085141 (2023)

<https://doi.org/10.1063/5.0165069>



View  
Online



Export  
Citation

CrossMark

## Articles You May Be Interested In

A functional integral formalism for quantum spin systems

*J. Math. Phys.* (July 2008)

# The effect of the cell tilting on the temperature oscillation in turbulent Rayleigh–Bénard convection

Cite as: Phys. Fluids **35**, 085141 (2023); doi: [10.1063/5.0165069](https://doi.org/10.1063/5.0165069)

Submitted: 26 June 2023 · Accepted: 10 August 2023 ·

Published Online: 29 August 2023



View Online



Export Citation



CrossMark

Xin Chen (陈鑫),<sup>1,2,a)</sup>  Ao Xu (徐翱),<sup>2</sup>  Ke-Qing Xia (夏克青),<sup>3</sup>  and Heng-Dong Xi (郗恒东)<sup>2,a)</sup> 

## AFFILIATIONS

<sup>1</sup>Shanghai Key Laboratory of Mechanics in Energy Engineering, Shanghai Institute of Applied Mathematics and Mechanics, School of Mechanics and Engineering Science, Shanghai University, Shanghai 200072, China

<sup>2</sup>School of Aeronautics and Institute of Extreme Mechanics, Northwestern Polytechnical University, Xi'an 710072, China

<sup>3</sup>Center for Complex Flows and Soft Matter Research and Department of Mechanics and Aerospace Engineering, Southern University of Science and Technology, Shenzhen 518055, China

<sup>a)</sup>Authors to whom correspondence should be addressed: [xinchen99@shu.edu.cn](mailto:xinchen99@shu.edu.cn) and [hengdongxi@nwpu.edu.cn](mailto:hengdongxi@nwpu.edu.cn)

## ABSTRACT

We experimentally studied the effect of cell tilting on the temperature oscillation in turbulent Rayleigh–Bénard convection. We simultaneously measured the temperature using both in-fluid and in-wall thermistors for  $Ra = 1.7 \times 10^9$  and  $5.0 \times 10^9$  at Prandtl number  $Pr = 5.3$ . The tilt angles relative to gravity are set to  $0^\circ$ ,  $0.5^\circ$ ,  $1^\circ$ ,  $2^\circ$ , and  $7^\circ$ . It is found that the temperature oscillation intensity measured in-fluid is much stronger than that measured in-wall, because the in-fluid thermistors measure both the large-scale circulation (LSC) and the plumes/plume clusters, while the in-wall thermistors only measure the LSC due to the filter effect of the sidewall. Despite the intensity difference, the obtained azimuthal profiles of the oscillation intensity measured by in-fluid and in-wall share similar spatial distribution, and the spatial distribution can be explained by the torsional motion near the top and bottom plates and the sloshing motion at the mid-height. With the in-fluid measurements, we find that with the increase in the tilt angle, the azimuthal profile of oscillation evolves toward a sawtooth-like profile and the intensity gets more prominent, which implies that the temperature oscillation becomes more coherent. Through a conditional sampling method based on the azimuthal position of LSC, we reveal that the uniformly distributed oscillation intensity in the level cell is the result of the superimposition of the random azimuthal motion and the sloshing motion. Tilting the cell can efficiently disentangle the above-mentioned two types of motions of LSC. Moreover, we found that the frequency of the temperature oscillation increases when the tilt angle increases, while the amplitude of the sloshing motion of the LSC remains unchanged, which is believed to be related to the confinement of the convection cell.

Published under an exclusive license by AIP Publishing. <https://doi.org/10.1063/5.0165069>

## I. INTRODUCTION

Thermal convection is a ubiquitous phenomenon in nature,<sup>1</sup> and it is also crucial for a wide range of industrial applications, such as cooling systems on chipboards.<sup>2</sup> A paradigm to study the generic convection is the Rayleigh–Bénard (RB) convection.<sup>3–7</sup> RB convection is a layer of fluid confined between two thermally conductive plates that are heated from below and cooled from above. The fluid is set in motion by the buoyancy when the applied temperature difference exceeds a critical value. The dynamics of the flow are determined by the geometry of the cell and two dimensionless parameters: the Rayleigh number  $Ra = \alpha g \Delta H^3 / (\nu \kappa)$  and the Prandtl number

$Pr = \nu / \kappa$ , where  $\Delta$  is the applied temperature difference,  $H$  is the height of the convection cell,  $g$  is the acceleration due to gravity, and  $\alpha$ ,  $\nu$ , and  $\kappa$  are the thermal expansion coefficient, kinematic viscosity, and thermal diffusivity of the fluid, respectively. The geometry of the convection cell is characterized by the aspect ratio  $\Gamma = D/H$ , where  $D$  is the diameter of the cylindrical cell. RB convection has attracted extensive investigations not only because it is a model system for studying buoyancy driving turbulence but also due to its importance in understanding the ubiquitous convection in nature, for example, convection in astrophysical and geophysical systems such as solar and mantle convection.<sup>1</sup>

A fascinating feature of the turbulent RB convection is the emergence of well-defined coherent oscillation in the presence of a turbulent background. This robust oscillation has been observed in both the temperature field<sup>8</sup> and velocity field<sup>9–11</sup> and in convection systems with different working fluids<sup>8,12–16</sup> and different geometries.<sup>17–20</sup> Qiu *et al.*<sup>9</sup> measured the velocity profile in a  $\Gamma = 1$  cell filled with water using laser Doppler velocimetry, and they found the mean flow field oscillates in a coherent manner. Similar velocity oscillations were observed in a  $\Gamma = 2$  cell.<sup>10,11</sup> Vogt *et al.*<sup>10</sup> attributed the velocity oscillation observed in low  $Pr$  liquid metal to a new “jump rope” flow mode, while Li *et al.*<sup>11</sup> discovered similar velocity oscillation in water, and they found the oscillation originates from the periodical orbiting of the vortex center. The geometry of the convection cell also significantly influences the occurrence of oscillations. For instance, in a cubic convection cell, Ji *et al.*<sup>20</sup> found that the large-scale circulation (LSC) aligns along the diagonal plane of the cell, which represents the longest path of the LSC. The temperature oscillation in this geometry originates from oscillation of the LSC orientation near the corner. Additionally, the size of the convection cell plays a role in the occurrence of oscillations. Qiu *et al.*<sup>21</sup> reported the onset of coherent oscillation and identified a critical  $Ra$  of  $5 \times 10^7$  for its occurrence. As  $Ra$  is proportional to the third power of the height of the convection cell, this critical  $Ra$  indicates a critical size of the oscillation. Regarding temperature oscillation, it exists in the temperature field measured in sidewalls,<sup>13,14,20,22–24</sup> in fluid,<sup>21,25–29</sup> and in bottom/top plate,<sup>8,25,27</sup> which seems to imply that temperature oscillation exists everywhere in the convection cell. A natural question is what the spatial structure of the temperature oscillation is and where those measured oscillating temperature signals are coming from. To answer the above questions, based on the temperature signals measured in the bottom plate,<sup>8</sup> Villermaux<sup>30</sup> first proposed that the oscillation is due to the periodic and alternate emission of thermal plumes from top and bottom boundary layers, which are coupled by the LSC. In this scenario, the arriving thermal plumes from the opposite plate impinge and disturb the boundary layer, and then the plume emission due to the boundary layer instability is triggered. This argument seems to be validated by some later experimental studies with temperature field measured in fluids<sup>26,28,31</sup> as well as the measured velocity field.<sup>31–33</sup> In addition to Villermaux’s physical model, Funfschilling and Ahlers<sup>34</sup> found that the frequency measured in the temperature or flow field corresponds to torsional motion of LSC near the top and bottom plates rather than the periodic plume emission. The discovery of torsional motion of LSC indicates that LSC has a rather intricate three-dimensional (3D) spatial structure and that it could be a complicated flow system with a characteristic frequency of a 3D flow motion. However, due to the up–down symmetry of the convection system, the torsional motion of the LSC should be canceled out at mid-height plane, which is inconsistent with the experiments measured at mid-height plane. With the complex 3D flow with characteristic frequency bearing in mind, Xi *et al.*<sup>27</sup> pointed out that the 3D measurements are essential to unlock the origin of temperature oscillations. We also note those experimental studies showing evidence of periodic plume emissions are mainly two-dimensional (2D) measurements.<sup>21,25,32,33</sup> Using 3D measurements of temperature field, Xi *et al.*<sup>27</sup> revealed that, in addition to the torsional motion, the LSC also undergoes the sloshing motion, and the sloshing and torsional motions together are responsible for the measured temperature and the velocity oscillations. Sloshing motion is a time-

periodic lateral displacement of the entire LSC plane away from cell center, and its behavior is more pronounced in the mid-height plane. The schematic diagrams of torsional and sloshing motion can be found in Brown and Ahlers.<sup>35</sup> Recently, Xie and Xia<sup>36</sup> experimentally studied the effect of the roughness surface on RBC, and they found that the roughness surface would increase the frequency of the temperature oscillation. Zwierner *et al.*<sup>15</sup> found that in a liquid metal convection system with low  $Pr$ , the twisting and sloshing motion also existed, and these two modes strongly influence the instantaneous heat transport.

Although the spatial structure of temperature oscillation had been studied extensively, the effect of the cell tilting on the temperature oscillation seems to be elusive. It has been widely studied that tilting of the convection cell could affect the heat transport,<sup>25,37–42</sup> flow dynamics,<sup>40–46</sup> and boundary layers.<sup>47</sup> Some results show that the heat transport remains almost unchanged or changes within 1% with increasing tilt angle,<sup>25,37,39</sup> while some other findings suggest that the heat transport can be decreased up to almost 5%.<sup>38,48</sup> However, for a wider range of tilt angle (up to  $90^\circ$ ), the relationship between heat transport and tilt angle becomes more complicated,<sup>40,44,49</sup> and it is found that the change of heat transport efficiency strongly depends on the flow topology. The cell tilting can significantly influence the flow dynamics. In cylindrical cell, it is found that the azimuthal motion of LSC is confined and LSC reversals are strongly inhibited.<sup>37</sup> In two-dimensional (2D) or quasi-2D geometry, for  $\Gamma = 1$ , tilt tends to suppress flow reversals while flow reversals are promoted by tilt for  $\Gamma = 2$ .<sup>43</sup> The effect of cell tilting on boundary layers had also been studied experimentally and showed that with different tilt angles, the shape of the normalized boundary layer profile is different.<sup>47</sup> Recently, Zhang *et al.*<sup>41</sup> introduced the concept of effective horizontal buoyancy, which provides a complete new point of view to study the convection with imperfect vertical alignment. Although much effort has been devoted to study the effect of cell tilting on various aspects of LSC, detailed study of the effect of cell tilting on temperature oscillation and its spatial structure in cylindrical cell is still lacking. Weiss and Ahlers<sup>39</sup> performed experiments in a cylindrical cell with  $\Gamma = 0.5$  and tilt angles up to  $0.12$  rad. They mainly focused on the torsional oscillation near the top and bottom plates and they found that the torsional oscillation becomes more pronounced and the oscillation frequency increased with increasing tilt angles. Guo *et al.*<sup>40</sup> experimentally studied the temperature oscillation in a rectangular cell over a wide range of tilt angle ( $0^\circ$ – $90^\circ$ ) and found that the oscillations exist in both temperature and velocity signals for almost all the tilt angles. The oscillation intensity of both temperature and velocity signals first increases with increasing tilt angle until it reach its maximum at around  $27.5^\circ$ , then it decreases as tilt angle further increases.

In this paper, we present a detailed experimental study on the effect of cell tilting on the temperature oscillation, particularly the sloshing motion, in a unit cylindrical RB convection cell using both in-fluid and in-wall thermistors. We first quantitatively compare the temperature signals simultaneously obtained by in-fluid and in-wall thermistors, and we can find that the direct contact between the fluid and thermistors leads to a much stronger oscillation strength. We define the oscillation intensity as the amplitude of power spectra at the corresponding oscillation frequency, and the azimuthal distribution of oscillation intensity is obtained under different tilt angles. In addition, we implement a conditional sampling method to the temperature time

series and successfully reveal the relationship between the sloshing motion and the azimuthal motion. Our study complements the understanding about the effect of cell tilting on temperature oscillation in RBC.

The rest of the paper is organized as follows: In Sec. II, we briefly present the experimental setup and methods. Section III includes the experimental results of comparison between temperature signals in fluid and sidewall, the spatial structure of the temperature oscillation, and the effect of tilting the cell. Discussion and the conclusions are presented in Sec. IV.

## II. EXPERIMENTAL SETUP AND METHODS

The experiments were conducted in a cylindrical convection cell that has been described in detail elsewhere.<sup>27,50,51</sup> Here, we only mention some key characteristics of the cell. The convection cell has a height of  $H = 19.0$  cm and a diameter of  $D = 19.0$  cm. It consists of an upper plate and a lower copper plate of thickness 1 cm with nickel-plated surfaces and a Plexiglas sidewall of thickness 0.5 cm. Water was used as the working fluid. The temperature of the system is measured by three sets of thermistors: the first set of thermistors are small thermistors with a diameter of  $300 \mu\text{m}$  (GE sensing), which are put inside the convection cell to measure the temperature of the fluid (denoted as  $T_f$ ); the second set of thermistors are big thermistors with a diameter of 2.5 mm (Omega 44031), which are embedded beneath the fluid-contact surface of each conducting plate to measure the temperature of the plate (denote as  $T_p$ ); the third set of thermistors are big thermistors that are put into the sidewall through blind-holes drilled from outside of the sidewall to measure its temperature (denoted as  $T_w$ ).

As shown in Fig. 1, the in-fluid small thermistors are mounted on a star-shaped frame made of stainless steel tube with diameter 1 mm. They are separated equally along the azimuthal position with a distance of 1 cm from the sidewall, where the main ascending and descending plumes pass through.<sup>32</sup> The frame is soldered perpendicularly to a stainless steel tube and can traverse vertically along the central axis of the convection cell. The thermistors are labeled as 1, 2, ..., 8, which also represent their azimuthal positions.

The large-scale flow is essentially an organized motion of thermal plumes,<sup>52</sup> in which the plumes carry hot (or cold) fluid when they flow up (or down) along the sidewall. Thus, the in-wall thermistors can feel and measure the convective flow inside the cell. Eight blind holes were drilled from the outside into the sidewall at the mid-height horizontal plane, and they were equally distributed and spaced azimuthally around the cylinder (see Fig. 1). The end of these holes are 0.7 mm away from the fluid-contact surface. Eight thermistors were placed into the eight blind holes until they touched the bottom snugly. To ensure good thermal contact, a thin layer of thermally conductive paste is spread around the surface of the thermistors. The temperatures in the top and bottom plates were measured by 16 big thermistors (see Fig. 1). Eight of them are embedded in the top plate at half radius from the plate center and about 2 mm away from the fluid contact interface at positions TP1 to TP8; while the other eight are similarly embedded in the bottom plate at positions BP1 to BP8. Each thermistor was calibrated with an accuracy of  $0.01^\circ\text{C}$ . The thermistors were connected to a  $6\frac{1}{2}$ -digit multichannel multimeter, and their resistances were measured at a sampling frequency of 0.29–0.67 Hz, which were then converted into temperatures using the calibration curves.

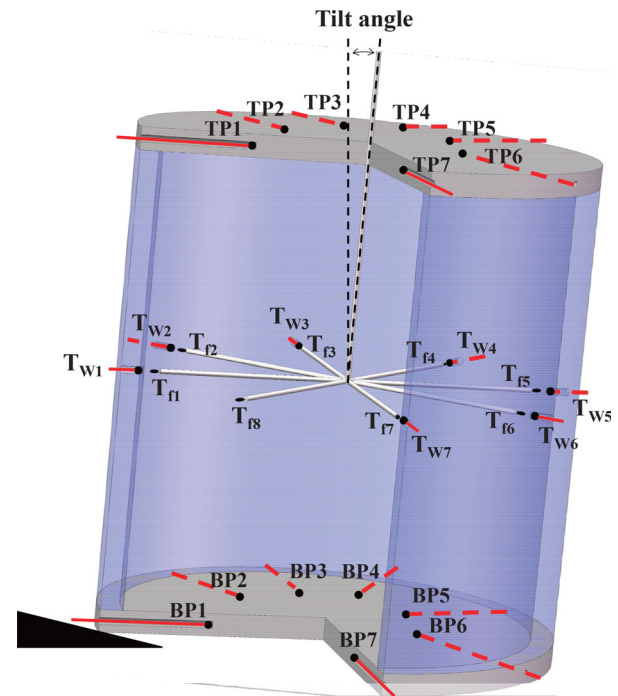


FIG. 1. Schematic illustration of the convection cell, positions of the small thermistors in fluid, and the big thermistors embedded in the sidewall and the plates. BP8 and TP8 are not shown. This sketch is adapted from Fig. 1(a) of Xi *et al.*<sup>27</sup>

The temperature measurements in fluid, in wall, and in plate are performed simultaneously unless stated otherwise. During the experiment, the entire cell is wrapped by several layers of styrofoam to avoid the heat exchange between the cell and the ambient environment. The measurements are carried out for  $Ra = 1.7 \times 10^9$  and  $5.0 \times 10^9$ , and the Prandtl number  $Pr$  is kept at 5.3. As the measurements for different  $Ra$  give the same qualitative results, thus, only results for  $Ra = 5.0 \times 10^9$  will be presented unless stated otherwise.

## III. RESULTS AND DISCUSSION

### A. The measured temperature signal in fluids and in sidewall

Figure 2 shows the segments of temperatures at the mid-height plane measured by the in-fluid and in-wall thermistors simultaneously. The convection cell is tilted by  $2^\circ$  at position 1. One can see the fluctuations of the in-fluid temperature are much more significant than those in the sidewall, in which the r.m.s. of the in-fluid temperature is about four times larger than that of the in-wall temperature. Because the sidewall acts as a low-pass filter, the thermistors embedded in the sidewall will only probe the low-frequency signal, and they spatially sense the integrated signal over a finite area of the sidewall (in other words, not individual plumes or clusters of plumes). Due to the thermal inertia or thermal mass of the sidewall, the in-wall thermistors measure an overall hotter or colder temperatures than the corresponding thermistors in-fluid. Therefore, the in-wall probes smooth out the temperature spikes that correspond to the individual plumes or plume clusters, and they are not sensitive in detecting the properties of

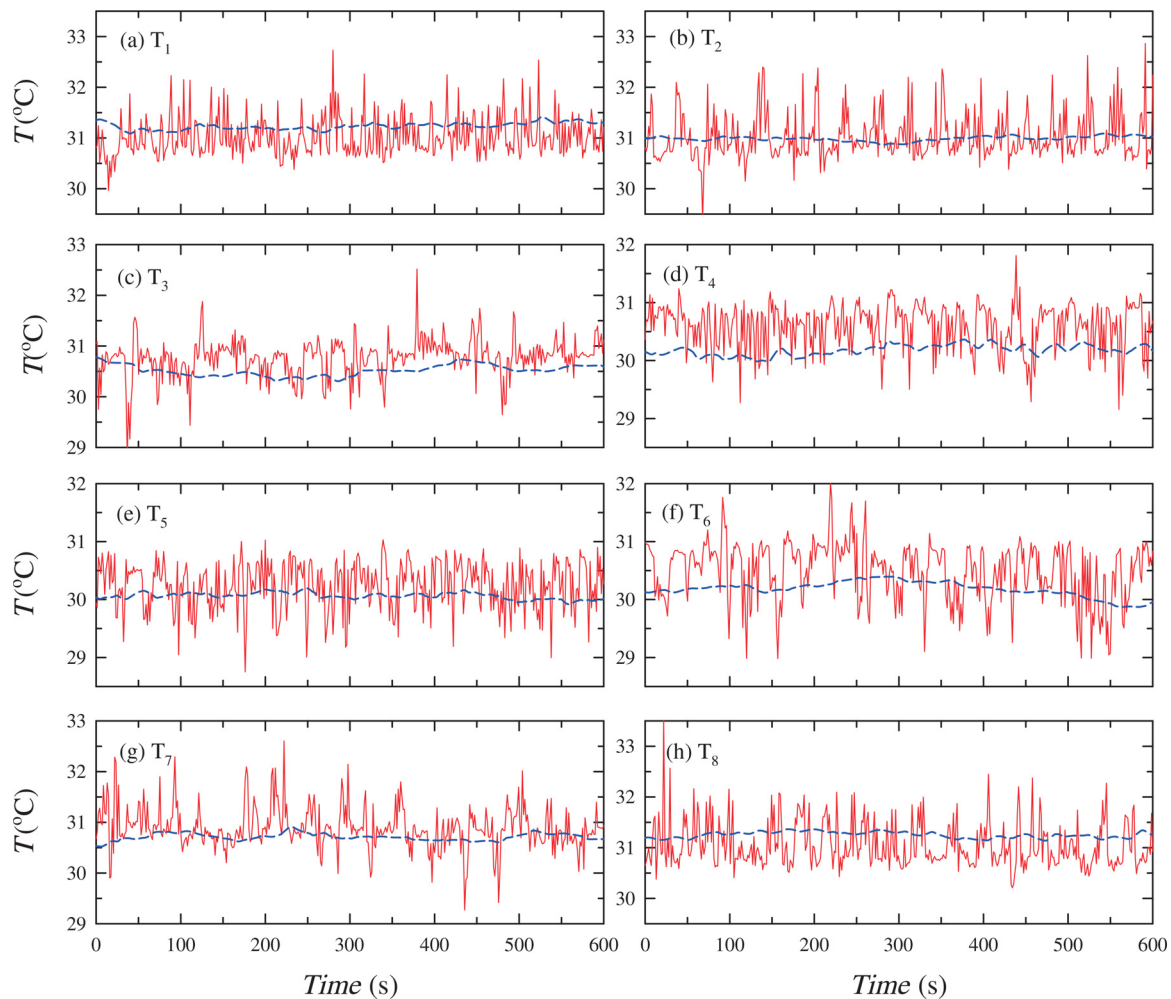


**FIG. 2.** Time traces of temperatures measured simultaneously by thermistors in fluid (red solid line) and in sidewall (blue dashed line) at the mid-height plane. Each of the in-fluid thermistors is 1 cm away from the sidewall, while each of the in-wall thermistors is 0.7 mm from fluid–sidewall interface. The convection cell is tilted by  $2^\circ$  at position 1.

plumes. At positions 1, 2, and 8, positive (hot) spikes are observed above the baseline, suggesting the presence of ascending hot plumes; at positions 4, 5, and 6, negative (cold) spikes are observed below the baseline, suggesting cold plumes are descending there; at positions 3 and 7, both positive (hot) spikes and negative spikes are present, implying both hot and cold plumes exist at these positions. These temperature signals are consistent with the coherent large-scale circulation that has a band of about half a diameter wide.

The properties of time trace shown in Fig. 2 are also manifested by the probability density functions (PDFs) of temperature traces. We can see that in Fig. 3(c), all the eight PDFs measured by in-fluid thermistors  $T_{f1} - T_{f8}$  fall under three groups. The PDFs of  $T_{f1}$ ,  $T_{f2}$ , and  $T_{f8}$  have fatter tails on the right, which are due to much more hot spikes. While the PDFs of  $T_{f4}$ ,  $T_{f5}$  and  $T_{f6}$  have fatter tails on the left, which are due to much more cold spikes. The PDFs of  $T_{f3}$  and  $T_{f7}$  are almost symmetric, indicating that hot and cold spikes have an equal probability of occurring. The peaks for all the eight PDFs are due to their corresponding average baselines. Figure 3(d) shows the PDFs of

the temperatures measured by eight in-wall thermistors. The eight PDFs, unlike that of the in-fluid temperatures, are symmetric and collapsed together, implying that the in-wall thermistors cannot sense the individual plume or plume clusters. In Figs. 3(a) and 3(b), we also show the PDFs of the temperatures in leveled cell measured by in-fluid thermistors and in-wall thermistors. Unlike the PDFs shown in Fig. 3(c), one can see from Fig. 3(a), the PDFs of the temperatures measured by in-fluid thermistors do not separate from each other and their tails collapsed together. The peaks of the eight PDFs slightly deviate from each other, and this is due to the fact that the residence time that LSC stays at different azimuthal positions is not identically equal during our experiments. If the acquisition time were much longer, we think that the PDFs of in-fluid thermistors in leveled cell would collapse and have the shape of  $T_{f3}$  and  $T_{f7}$  shown in Fig. 3(c). The PDFs will be almost symmetric, indicating that hot and cold spikes have an equal probability. However, we believe that the PDFs will not recover a Gaussian shape for the in-fluid thermistors. In previous study, Zhou *et al.*<sup>53</sup> found that the measured temperature signal profile of a plume

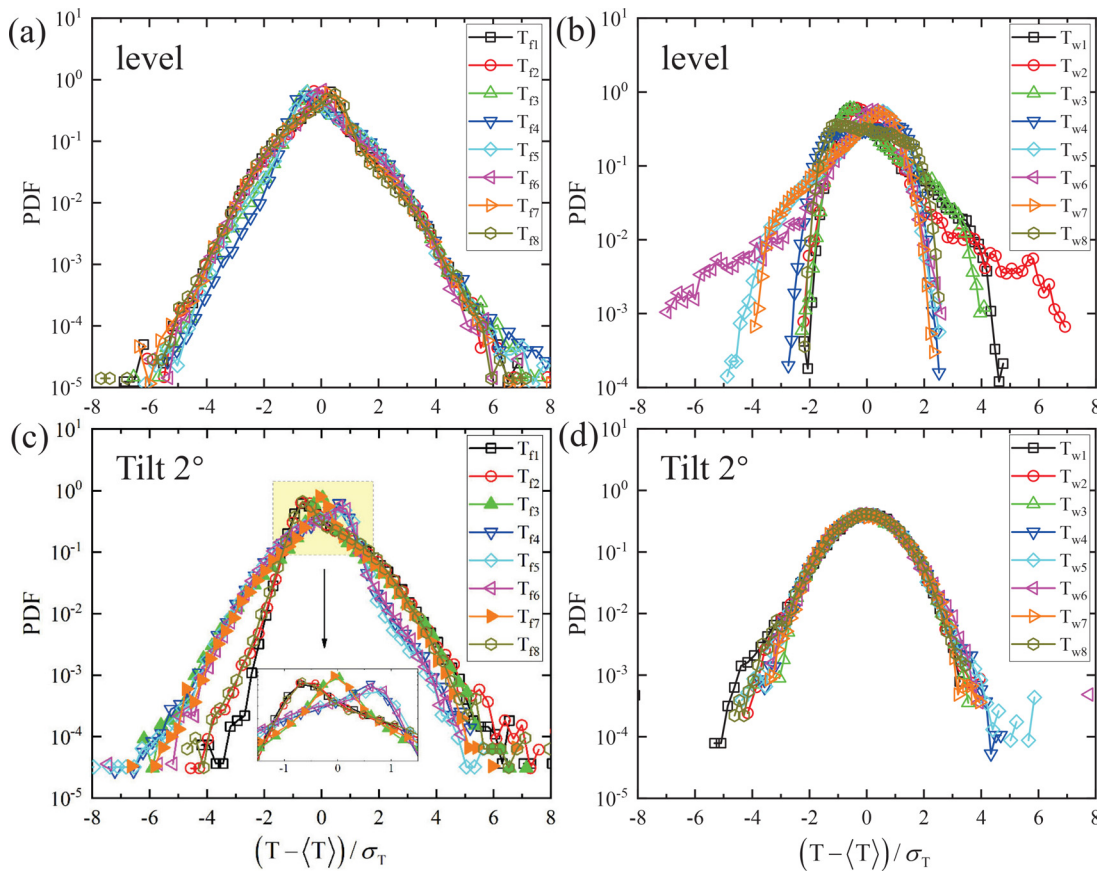


**FIG. 3.** Probability density functions (PDFs) of the temperature measured at the mid-height horizontal plane by the eight in-fluid thermistors (a) and (c) and the eight in-wall thermistors (b) and (d). The convection cell is leveled for (a) and (b) and is tilted by  $2^\circ$  at position 1 for (c) and (d). In (c), the inset displays a magnified view of the data within the rectangular region.

passing the thermistor is not symmetric. The asymmetric temperature signals could lead a deviation from a Gaussian shape. In contrast to the symmetric, well-collapsed, Gaussian PDFs, which are shown in Fig. 3(d), in Fig. 3(b), the PDFs of the temperatures in leveled cell measured by in-wall thermistors have a more complicated form. Each PDF has wider distribution than that in a tilted cell, which indicates that the LSC undergoes a random azimuthal motion. If the acquisition time were much longer, we believe that it will eventually recover a Gaussian shape as that in Fig. 3(d).

In Fig. 4, we show the power spectra of temperatures measured simultaneously at mid-height horizontal plane by both in-fluid and in-wall thermistors. The convection cell is tilted by  $2^\circ$  at position 1. First, one can see that the power spectra of in-wall temperatures decay faster than that of in-fluid temperatures over the frequency range, especially at high frequency range, which further quantitatively confirms that the sidewall is a low-pass filter, i.e., the high frequency signal (individual plumes or clusters) is filtered out by the sidewall. Also, we can see the prominent peaks in both power spectra. The prominent peaks in the power spectra locate at the frequency of the temperature oscillation, which are consistent with previous observations.<sup>8,23,27</sup> The intensity of the oscillations can be quantified by the peak height  $P(f_0)$  of the power

spectra at  $f_0$ . Figure 4(d) plots the azimuthal profile of  $P_0$  measured at mid-height of the cell by both in-fluid and in-wall thermistors. We can see that there are no significant oscillations at positions 1 and 5 (i.e., within the circulation plane of the LSC), neither at positions 3 and 7 (i.e., out of the circulation plane of the LSC). On the other hand, strong oscillations are presented at positions 2, 4, 6, and 8, which is due to the sloshing motion of the LSC.<sup>23,27</sup> To have the spatial structure of the temperature oscillation, we traverse the eight in-fluid thermistors vertically to heights of  $H/4$  and  $3H/4$  and repeat the measurements. Figures 4(c) and 4(e) show the azimuthal distribution of the oscillation strength  $P_0$  obtained at these heights, respectively. It has been shown previously that the LSC undergoes horizontal twisting oscillation near the top and bottom plates,<sup>22,24,34</sup> and the strong oscillations at positions 4 and 6 at  $3/4H$ , positions 2 and 8 at  $1/4H$  essentially reflect this motion. In Fig. 4(d), the profile of  $p(f_0)$  measured by in-wall thermistors is also plotted. From the value of right vertical axis, one can see that the amplitude of oscillation strength is much weaker than that of in-fluid measurements. The much stronger oscillation strength is understandable as the in-fluid thermistors are directly in contact with the working fluid. Hence, in what follows, unless stated otherwise, only the temperature results measured by in-fluid thermistors will be presented.

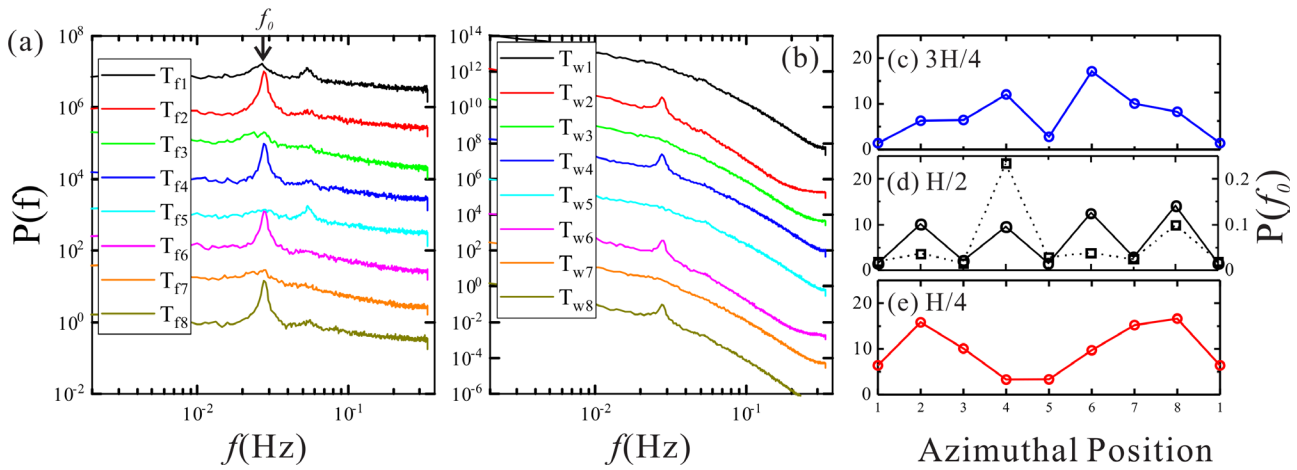


**FIG. 4.** The convection cell is tilted by  $2^\circ$  at position 1. From top to bottom: power spectra of the temperatures measured at the mid-height horizontal plane at the positions 1–8 by the in-fluid thermistors (a) and in-wall thermistors (b). For clarity, each dataset is shifted upward from its lower neighbor by a constant factor. It should be noted that (a) was previously presented in Xi *et al.*;<sup>27</sup> here, we replot it for comparison. (c)–(e) The azimuthal profiles of the temperature oscillation strength  $P(f_0)$  measured at the  $3H/4$ ,  $H/2$ , and  $H/4$  horizontal planes, respectively. Here, the  $f_0$  is the frequency of the power spectra peak shown in (a) and (b). In (d), the  $p(f_0)$  profile measured by in-wall thermistors is also plotted in dashed line for comparison, and the point value corresponds to the right vertical axis.

**B. The effects of tilting the cell**

In the above results, the cell is tilted by  $2^\circ$ , and there is clear temperature oscillation in the central part (due to sloshing motion of the LSC) and near boundary layers of the convection cell (due to the torsional oscillation). When the cell is tilted by a small angle, the LSC is confined in a smaller azimuthal range; while the cell is leveled, the LSC’s vertical plane undertakes azimuthal motion in a Brownian motion manner.<sup>37,45</sup> A natural question arises: what is the behavior of temperature oscillation in a leveled cell, and how does the cell tilting affect the temperature oscillation? In Fig. 5(c), we show the r.m.s. of the orientation of the LSC measured at the mid-height  $\sigma_\phi$  as a function of the tilt angle of the cell. The fact that  $\sigma_\phi$  decreases rapidly with increasing tilt angle indicates that for larger tilt angle, the LSC is confined in a smaller azimuthal range. This result is consistent with that obtained by Ahlers *et al.*<sup>45</sup> Because the LSC explores a larger azimuthal region ( $\sigma_\phi = 40^\circ$ ) in a level cell than that in a tilted cell ( $\sigma_\phi = 8.5^\circ$ ),

we expect that the azimuthal motion of the LSC plays a more important role in a leveled cell. In Fig. 5(a), we plot the power spectra of the  $T_{f1}$  to  $T_{f8}$  when the cell is level (i.e., tilt angle of  $0^\circ$ ). We found that strong temperature oscillations occur at all eight positions. The corresponding azimuthal profile of the oscillation intensity is further shown in Fig. 5(b), and we can see that when the cell is leveled, the oscillation intensity is almost equally distributed azimuthally. However, in this level case, the strength of oscillation [the peak height of power spectra,  $p(f_0)$ ] is reduced as compared to the tilted case.

One may argue that whether the “jump rope” flow mode revealed by Vogt *et al.*<sup>10</sup> also exists in current  $\Gamma = 1$  convection cell since the temperature oscillation shown in Fig. 5(a) is quite similar to that of the “jump rope” flow mode. The “jump rope” flow mode has a dominant 3D vortex core that orbits in the cell periodically, and it travels in the direction opposite to that of the LSC (see Fig. 1 in Vogt *et al.*<sup>10</sup>), thus, generating intense temperature and velocity oscillation

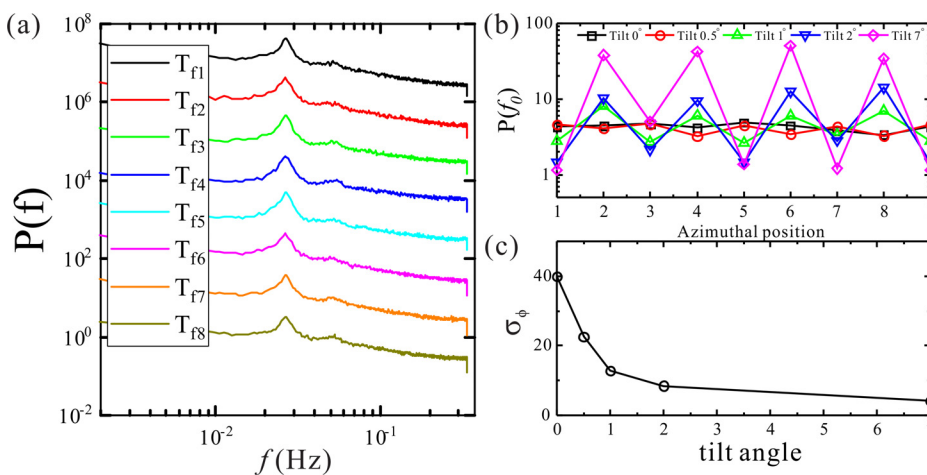


**FIG. 5.** The convection cell is leveled. (a) From top to bottom: power spectra of the temperatures measured at the mid-height horizontal plane at the positions 1–8 by the in-fluid thermistors. Also, the power spectra of the circumferentially averaged temperature signal  $T_{r,all} = (\sum_{i=1}^8 T_{fi})/8$ . For clarity, each dataset is shifted upward from its lower neighbor by a constant factor. (b) The azimuthal profiles of the temperature oscillation strength  $P(f_0)$  measured in fluid at mid-height for different tilt angles. (c) RMS of the orientation ( $\phi$ ) of the LSC  $\sigma_\phi$  at different tilt angles.

29 August 2023 14:03:19

everywhere in the convection cell, including the bulk and the periphery region of the cell. In the periphery region, they found that the strong temperature oscillation exists everywhere, regardless of whether the probes are in the LSC plane or not. Figure 5 in Vogt *et al.*<sup>10</sup> showed that the calculated circumferentially averaged temperature signal  $T_{\text{avg}}$  at mid-height and  $T_{\text{avg}}$  exhibits a well-defined quasi-periodic oscillation. Here, in Fig. 5(a), we also plot the power spectra of  $T_{f,\text{all}}$ , which is the circumferentially averaged temperature signal of in-fluid thermistors. Apparently, there is no obvious peak in that power spectra. In addition, a previous study<sup>26</sup> had shown that in unity cylindrical cell, the temperature oscillation can only be detected in the region where vast plumes travel through and there is no sign of temperature oscillation observed in the center of  $\Gamma = 1$  convection cell. Thus, we think the “jump rope” flow mode does not exist in our current experiments, and it cannot be used to explain Fig. 5(a).

The reason to explain Fig. 5(a) is that the azimuthal meandering is superimposed with the sloshing motion. Due to the strong azimuthal motion, the LSC band could leave the (1,5) plane and, for example, align with (2,6) plane, then the thermistors 1, 3, 5, and 7 could measure the periodical temperature signals; similarly, the LSC band could align with (3, 7) plane and (4, 8) plane as well. On the contrary, when the cell is tilted with a large angle, sloshing motion is predominant than the azimuthal meandering. Thus, the LSC could only leave and return to the (1,5) plane, and only the thermistors 2, 4, 6, and 8 could measure the periodical temperature changes. Thus, the profile is a sawtooth-like distribution for large tilt angles of  $1^\circ$ ,  $2^\circ$ , and  $7^\circ$ , as shown in Fig. 5(b). Meanwhile, the amplitude of the sawtooth-like profile gets pronounced with the increase in tilt angles.

In Fig. 6, we show the auto-correlation functions of the off-center distance  $d_{oc}$  measured by in-fluid thermistors for different tilt angles. Well-harmonic curves can be found for all cases, especially for the large tilt cases, i.e.,  $7^\circ$  case. The amplitude of well-harmonic curve, namely the value of  $C(\tau)$ , increases with the increase in the tilt angle. The coherence time for each tilt angle can be simply quantified by counting how many oscillation cycles<sup>21</sup> are in Fig. 6. There are roughly

seven oscillation cycles for the leveled case. With the increase in tilt angles, the number of oscillation cycles increases monotonically. For tilt  $7^\circ$  case, the well-harmonic shape oscillation cycles can still be found beyond 2000 s. Combining the sharper triangles shown in Fig. 5 and the well-harmonic oscillation cycles shown in Fig. 6, one can conclude that the sloshing motion is getting more coherent at larger tilt angles.

The relationship between the sloshing motion and azimuthal meandering can be revealed by the cross correlation functions between temperatures measured at the opposite azimuthal position. In Figs. 7(a)–7(c), we show the cross correlation functions at different tilt angles. For level and slightly tilted case of  $0.5^\circ$ , we found all four pairs of temperature series show similar and well-defined correlations. This kind of correlation was also suggested by some earlier measurements made in a 2D plane, that the thermal plumes are emitted periodically. Now it is clear that the periodicity is not due to the periodic plume emission, but by the combination of sloshing and the azimuthal meandering of LSC. When the cell is tilted by  $2^\circ$ , the LSC is locked steadily in a minimal azimuthal range, the alternate appearance of hot and cold plumes at positions 1 and 5 is absent as well as at positions 3 and 7.

To disentangle the azimuthal motion and slosh motion of LSC, the ideal approach is to keep the cell level and move the eight thermistors azimuthally with the LSC's orientation plane in a synchronized way. In practice, we will keep the cell leveled and only account those measurements when the LSC's orientation is within a small angular range centered on its preferred orientation. Here, we assume that the preferred orientation of the LSC happens to be in the (2,6) vertical plane. To consider the motions of the flow only when LSC is in the (2,6) plane, we set  $T_i(t) = \langle T_i \rangle$ ,  $i = 1, 2, \dots, 8$  when LSC's orientation is outside its preferred orientation angle plus/minus  $10^\circ$ . Figure 8 further shows the power spectra of the resultant time traces for both in-fluid and in-wall temperatures. If we compare the above result with that shown in Fig. 4(a), we can observe the very same behavior except that the oscillations are not as sharp as that in the tilted case. Indeed, the phase relationships of the oscillations observed at different positions are also the same as the tilted case, which is shown by the cross correlation functions in Fig. 7. Figures 7(c) and 7(d) show the cross correlation functions calculated by the tilted case dataset and selected dataset, respectively. It should be noted that the (1,5) plane in the tilted case is equivalent to the (2,6) plane in the conditional data for the leveled case, as we can observe the same behavior (for example, the correlation between  $T_3$  and  $T_7$  is the same as that between  $T_2$  and  $T_6$  in the tilted case). These results also indicate that the conclusions from the present work do not depend on the tilting of the cell, and tilting the cell just disentangles different aspects of the convective flow.

Figure 9(a) shows the PDFs of off-center distance  $d_{oc}/D$  obtained from in-wall thermistors for both the leveled and  $7^\circ$  tilted cases. One can see that for the tilted case, the PDF has a narrower distribution range than that of the leveled case. Also, the PDF shape around its mean value of 0 is flatter than that of the leveled case. The reason for the observed different distributions for the leveled and tilted cases is, when the cell is tilted, see the schematic drawing of Fig. 9(b), that the LSC is confined in a fixed orientation; thus, the LSC plane can only slosh around a fixed vertical plane of the cell, and it is reasonable to see that the PDF of  $d_{oc}/D$  is more concentrated. When the cell is leveled, the LSC undergoes the sloshing motion along with the random

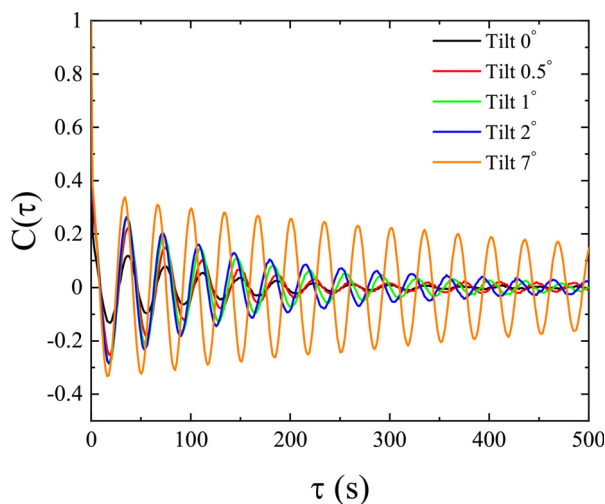
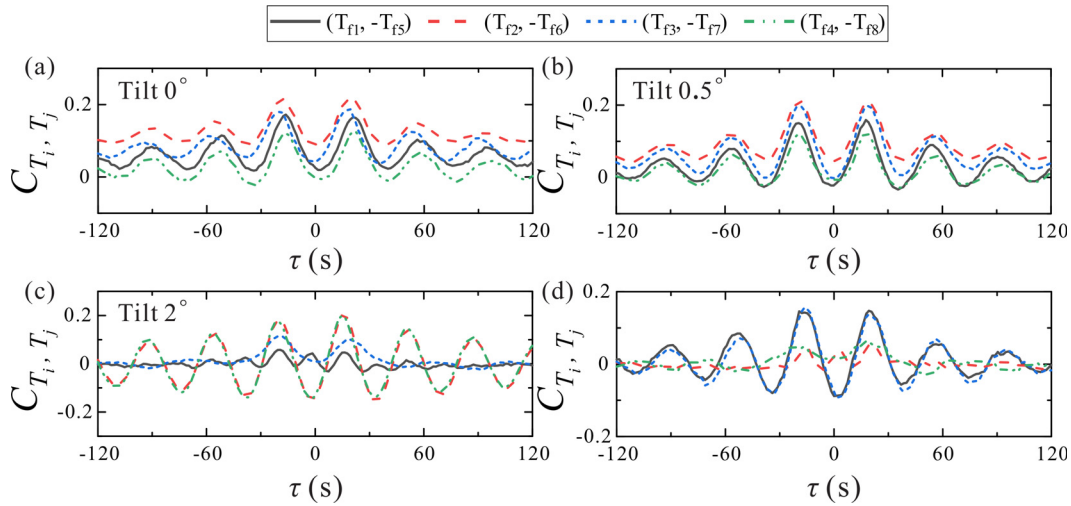


FIG. 6. The auto-correlation functions of the off-center distance  $d_{oc}$  measured by in-fluid thermistors for different tilt angles.





**FIG. 7.** The cross correlation functions between temperatures measured by in-fluid thermistor pairs placed at opposite positions: (a) the cell is leveled; (b) the cell is tilted by  $0.5^\circ$  at position 1; (c) the cell is tilted by  $2^\circ$  at position 1; and (d) as in (a) but the temperature data  $T_i(t)$  when the LSC is not in (2,6) plane is set to a constant value of  $\langle T_i \rangle$ , ( $i = 1, 2, \dots, 8$ ) to mimic the case that the LSC is locked in the (2,6) plane.

azimuthal meandering. If the LSC plane rotates counterclockwise, see the schematic drawing of Fig. 9(c), the value of  $d_{OC}/D$  becomes larger compared to that of the tilted case, and if the LSC plane rotates clockwise, the off-center distance becomes smaller. Under this circumstance, the probabilities of larger or smaller  $d_{OC}$  is higher than that of the tilted case. Here, we do not show the PDFs of  $d_{OC}/D$  measured by in-fluid thermistors because the PDFs do not change with cell tilting and are similar to previous results.<sup>23</sup> The unchanged PDFs of  $d_{OC}/D$  measured in-fluid are due to the fact that the in-fluid thermistors have a higher sensitivity to measure the sloshing motion of LSC since they can capture the passing of individual or clusters of plumes as we discussed in Sec. III A.

The temperature oscillation frequency and off-center distance as functions of the tilt angle is shown in Fig. 10. We can see that the frequency of the temperature oscillation increases when the tilt angle increases, while the off-center distance (amplitude) of the sloshing

motion of the LSC remains almost unchanged. Combining Fig. 5(b), we can conclude that with the increase in tilt angle, the coherence and the frequency of temperature oscillation (sloshing motion) increase. The unchanged off-center distance, which is similar to the  $Ra$  dependence of the off-center distance,<sup>23</sup> may result from the limited space of the cylindrical geometry for the LSC to explore itself, since the LSC expands almost half the diameter of the cell.<sup>27</sup>

**IV. CONCLUSIONS**

In this work, a systematic experimental study on the spatial structure of temperature oscillation and the effects of cell tilting had been carried out in a unit cylindrical Rayleigh–Bénard convection cell. Simultaneous measurements of the temperatures in fluid and in sidewall were taken for different tilt angles. We found that the sidewall acts like a low-pass filter: the temperature signals measured from sidewall are only affected by the LSC, while the temperature signals

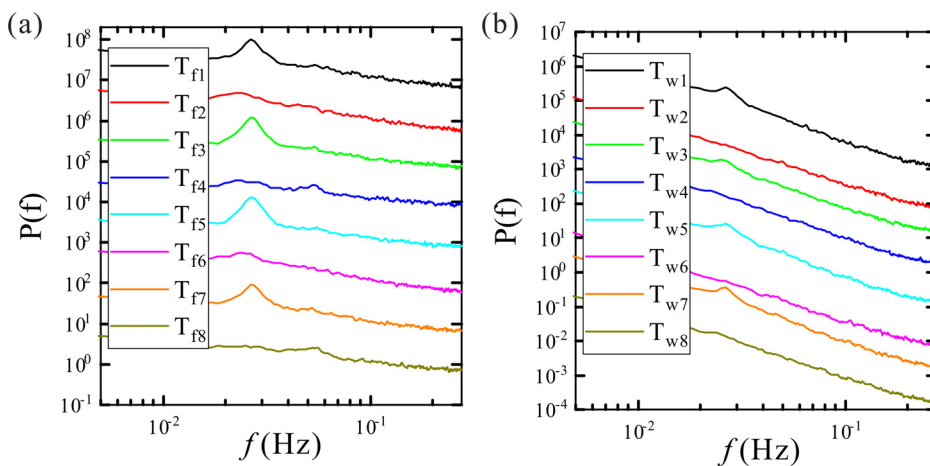


**FIG. 8.** Power spectra of the temperatures measured by eight in-fluid thermistors (a) and in-wall thermistors (b) at mid-height plane. Here, the cell is leveled, the temperature data  $T_i(t)$  when the LSC is not in (2,6) plane is set to a constant value of  $\langle T_i \rangle$ , ( $i = 1, 2, \dots, 8$ ) to mimic the case that the LSC is locked in the (2,6) plane.

29 August 2023 14:03:19

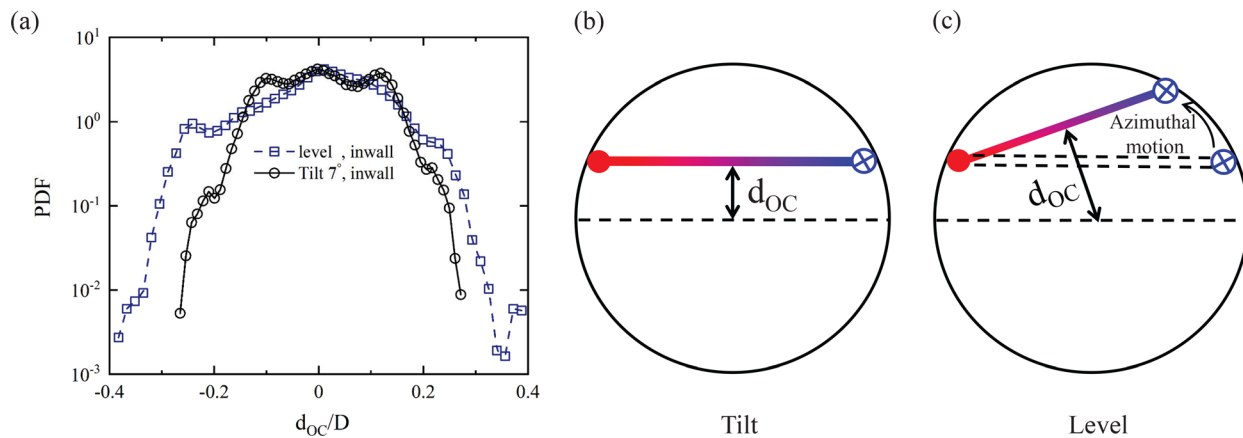


**FIG. 9.** (a) Probability density functions (PDFs) of the off-center distance  $d_{OC}$  measured by in-wall thermistors. The convection cell is leveled for square symbols and is tilted by  $7^\circ$  for cycle symbols. It should be noted that the PDF of the leveled case was previously presented in Zhou *et al.*;<sup>23</sup> here, we plot it for comparison. (b) and (c) are the schematic drawings of the off-center motion of the LSC at a tilted cell and a leveled cell.

measured in-fluid are affected by both the LSC and travel-by plumes. Despite the difference of the temperature signals, the temperature measured in-fluid and in sidewall both show strong oscillations and exhibit similar temperature oscillation spatial structure. The results above suggest that the LSC, rather than the plumes, plays a key role in the oscillatory motion.

The spatial structure of temperature oscillation is manifested by the azimuthal profiles of temperature oscillation strength measured at different heights. At  $H/4$  and  $3H/4$ , azimuthal profiles of temperature oscillation strength are well explained by the torsional motion of the LSC near the top and the bottom plates; while at  $H/2$ , the azimuthal profile of the temperature oscillation strength can be well explained by the sloshing motion perpendicular to the LSC plane.

Although cell tilting, a commonly used approach to lock the LSC, had been studied extensively for decades, the effect of cell tilting on the temperature oscillation remained elusive previously, especially on the sloshing motion of the LSC. In our work, we find that when the cell is leveled or slightly tilted (less than  $1^\circ$ ), the temperature oscillation can

be detected at all eight positions at mid-height. The combination of azimuthal meandering and sloshing motion leads to the temperature oscillation at any spatial position, this is the case of most previous studies where oscillation of temperature was found everywhere because the cell was level or was only slightly tilted. When the cell is tilted, the azimuthal meandering is suppressed, and the sloshing motion becomes predominant. That is why the sawtooth distribution of temperature oscillation emerges. The sawtooth oscillation profile becomes more pronounced with the increase in tilt angle, which indicates a more coherent oscillation. With a conditional sampling method based on the azimuthal position of LSC, we reveal that the cell tilting can disentangle the azimuthal motion and the sloshing motion efficiently. This disentanglement enabled us to further confirm that the origin of the temperature oscillation is the torsional motion and sloshing motion, rather than the alternate and periodic emission of thermal plumes. Moreover, we also found that with the increase in tilt angle, the frequency of the temperature oscillation increases, while the off-center distance induced by the sloshing motion remains unchanged.

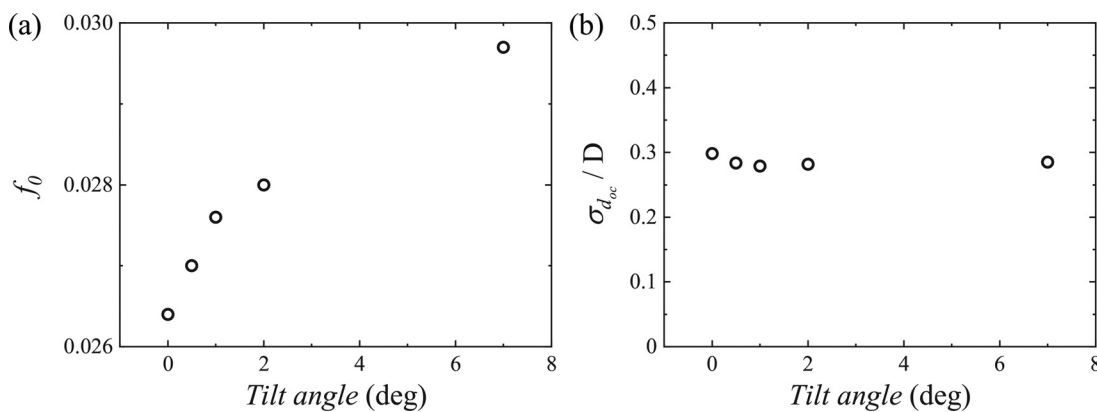


**FIG. 10.** (a) The frequency of the temperature oscillation as functions of the tilt angle. (b) The r.m.s. of the off-center distance of the sloshing motion as a function of the tilt angle.

29 August 2023 14:03:19

Our findings provide a significant step toward better understanding that the temperature oscillation originates from the bulk flow rather than the boundary layer and thus contribute to the establishment of a theoretical framework concerning the dynamics of LSC in turbulent thermal convection.

## ACKNOWLEDGMENTS

This work was supported by the National Natural Science Foundation of China (NSFC) under Grant No. 12125204, the China Postdoctoral Science Foundation under Grant No. 2021M702077, and the 111 Project of China (No. B17037). The experiment was conducted at the Chinese University of Hong Kong.

## AUTHOR DECLARATIONS

### Conflict of Interest

The authors have no conflicts to disclose.

## Author Contributions

**Xin Chen:** Conceptualization (equal); Investigation (equal); Methodology (equal); Writing – original draft (equal); Writing – review & editing (equal). **Ao Xu:** Conceptualization (equal); Investigation (equal); Methodology (equal); Writing – review & editing (equal). **Keqing Xia:** Conceptualization (equal); Supervision (equal); Writing – review & editing (equal). **Heng-Dong Xi:** Conceptualization (equal); Funding acquisition (equal); Investigation (equal); Supervision (equal); Writing – review & editing (equal).

## DATA AVAILABILITY

The data that support the findings of this study are available from the corresponding author upon reasonable request.

## REFERENCES

- L. P. Kadanoff, “Turbulent heat flow: Structures and scaling,” *Phys. Today* **54**(8), 34–39 (2001).
- X.-Q. Guo, B.-F. Wang, J.-Z. Wu, K.-L. Chong, and Q. Zhou, “Turbulent vortical convection under vertical vibration,” *Phys. Fluids* **34**, 055106 (2022).
- G. Ahlers, S. Grossmann, and D. Lohse, “Heat transfer and large scale dynamics in turbulent Rayleigh-Bénard convection,” *Rev. Mod. Phys.* **81**, 503–537 (2009).
- D. Lohse and K.-Q. Xia, “Small-scale properties of turbulent Rayleigh-Bénard convection,” *Annu. Rev. Fluid Mech.* **42**, 335–364 (2010).
- F. Chilla and J. Schumacher, “New perspectives in turbulent Rayleigh-Bénard convection,” *Eur. Phys. J. E* **35**, 58 (2012).
- K.-Q. Xia, “Current trends and future directions in turbulent thermal convection,” *Theor. Appl. Mech. Lett.* **3**, 052001 (2013).
- Y.-C. Xie, L. Zhang, G.-Y. Ding, X. Chen, H.-D. Xi, and K.-Q. Xia, “Progress in turbulent thermal convection in the past decade and outlook,” *Adv. Mech.* **53**, 1–47 (2023) (in Chinese).
- B. Castaing, G. Gunaratne, F. Heslot, L. P. Kadanoff, A. Libchaber, S. Thomae, X.-Z. Wu, S. Zaleski, and G. Zanetti, “Scaling of hard thermal turbulence in Rayleigh-Bénard convection,” *J. Fluid Mech.* **204**, 1–30 (1989).
- X.-L. Qiu, S.-H. Yao, and P. Tong, “Large-scale coherent rotation and oscillation in turbulent thermal convection,” *Phys. Rev. E* **61**, R6075 (2000).
- T. Vogt, S. Horn, A. M. Grannan, and J. M. Aurnou, “Jump rope vortex in liquid metal convection,” *Proc. Natl. Acad. Sci. U. S. A.* **115**, 12674–12679 (2018).
- Y.-Z. Li, X. Chen, A. Xu, and H.-D. Xi, “Counter-flow orbiting of the vortex centre in turbulent thermal convection,” *J. Fluid Mech.* **935**, A19 (2022).
- T. Takeshita, T. Segawa, J. A. Glazier, and M. Sano, “Thermal turbulence in mercury,” *Phys. Rev. Lett.* **76**, 1465 (1996).
- E. Brown, D. Funfschilling, and G. Ahlers, “Anomalous Reynolds-number scaling in turbulent Rayleigh-Bénard convection,” *J. Stat. Mech.* **2007**, P10005.
- P. Wei, “Large-scale circulation and oscillation in turbulent Rayleigh-Bénard convection with a Prandtl number  $Pr = 12.3$ ,” *AIP Adv.* **11**, 015111 (2021).
- L. Zwirner, R. Khalilov, I. Kolesnichenko, A. Mamykin, S. Mandrykin, A. Pavlinov, A. Shestakov, A. Teimurazov, P. Frick, and O. Shishkina, “The influence of the cell inclination on the heat transport and large-scale circulation in liquid metal convection,” *J. Fluid Mech.* **884**, A18 (2020).
- X. Zheng, S.-H. Xin, M. Boutaous, C. Wang, D. A. Siginer, and W.-H. Cai, “Oscillating onset of the Rayleigh-Bénard convection with viscoelastic fluids in a slightly tilted cavity,” *Phys. Fluids* **35**, 023107 (2023).
- J. J. Niemela and K. R. Sreenivasan, “Turbulent convection at high Rayleigh numbers and aspect ratio 4,” *J. Fluid Mech.* **557**, 411 (2006).
- R. du Puits, C. Resagk, and A. Theiss, “Breakdown of wind in turbulent thermal convection,” *Phys. Rev. E* **75**, 016302 (2007).
- S.-Q. Zhou, C. Sun, and K.-Q. Xia, “Measured oscillations of the velocity and temperature fields in turbulent Rayleigh-Bénard convection in a rectangular cell,” *Phys. Rev. E* **76**, 036301 (2007).
- D.-D. Ji and E. Brown, “Oscillation in the temperature profile of the large-scale circulation of turbulent convection induced by a cubic container,” *Phys. Rev. Fluids* **5**, 063501 (2020).
- X.-L. Qiu and P. Tong, “Onset of coherent oscillations in turbulent Rayleigh-Bénard convection,” *Phys. Rev. Lett.* **87**, 094501 (2001).
- H.-D. Xi and K.-Q. Xia, “Azimuthal motion, reorientation, cessation, and reversal of the large-scale circulation in turbulent thermal convection: A comparative study in aspect ratio one and one-half geometries,” *Phys. Rev. E* **78**, 036326 (2008).
- Q. Zhou, H.-D. Xi, S.-Q. Zhou, C. Sun, and K.-Q. Xia, “Oscillations of the large-scale circulation in turbulent Rayleigh-Bénard convection: The sloshing mode and its relationship with the torsional mode,” *J. Fluid Mech.* **630**, 367 (2009).
- D. Funfschilling, E. Brown, and G. Ahlers, “Torsional oscillations of the large-scale circulation in turbulent Rayleigh-Bénard convection,” *J. Fluid Mech.* **607**, 119 (2008).
- S. Ciliberto, S. Cioni, and C. Laroche, “Large-scale flow properties of turbulent thermal convection,” *Phys. Rev. E* **54**, R5901 (1996).
- X.-L. Qiu and P. Tong, “Temperature oscillations in turbulent Rayleigh-Bénard convection,” *Phys. Rev. E* **66**, 026308 (2002).
- H.-D. Xi, S.-Q. Zhou, Q. Zhou, T.-S. Chan, and K.-Q. Xia, “Origin of the temperature oscillation in turbulent thermal convection,” *Phys. Rev. Lett.* **102**, 044503 (2009).
- H. Song, E. Villermaux, and P. Tong, “Coherent oscillations of turbulent Rayleigh-Bénard convection in a thin vertical disk,” *Phys. Rev. Lett.* **106**, 184504 (2011).
- D. Schmeling, J. Bosbach, and C. Wagner, “Oscillations of the large-scale circulation in turbulent mixed convection in a closed rectangular cavity,” *Exp. fluids* **54**, 1517 (2013).
- E. Villermaux, “Memory-induced low frequency oscillations in closed convection boxes,” *Phys. Rev. Lett.* **75**, 4618–4621 (1995).
- X.-L. Qiu, X.-D. Shang, P. Tong, and K.-Q. Xia, “Velocity oscillations in turbulent Rayleigh-Bénard convection,” *Phys. Fluids* **16**, 412 (2004).
- C. Sun, K.-Q. Xia, and P. Tong, “Three-dimensional flow structures and dynamics of turbulent thermal convection in a cylindrical cell,” *Phys. Rev. E* **72**, 026302 (2005).
- Y. Tsuji, T. Mizuno, T. Mashiko, and M. Sano, “Mean wind in convective turbulence of mercury,” *Phys. Rev. Lett.* **94**, 034501 (2005).
- D. Funfschilling and G. Ahlers, “Plume motion and large-scale circulation in a cylindrical Rayleigh-Bénard cell,” *Phys. Rev. Lett.* **92**, 194502 (2004).
- E. Brown and G. Ahlers, “The origin of oscillations of the large-scale circulation of turbulent Rayleigh-Bénard convection,” *J. Fluid Mech.* **638**, 383–400 (2009).
- Y.-C. Xie and K.-Q. Xia, “Turbulent thermal convection over rough plates with varying roughness geometries,” *J. Fluid Mech.* **825**, 573–599 (2017).

- <sup>37</sup>S. Cioni, S. Ciliberto, and J. Sommeria, “Strongly turbulent Rayleigh-Bénard convection in mercury: Comparison with results at moderate Prandtl number,” *J. Fluid Mech.* **335**, 111–140 (1997).
- <sup>38</sup>C. Sun, H.-D. Xi, and K.-Q. Xia, “Azimuthal symmetry, flow dynamics, and heat transport in turbulent thermal convection in a cylinder with an aspect ratio of 0.5,” *Phys. Rev. Lett.* **95**, 074502 (2005).
- <sup>39</sup>S. Weiss and G. Ahlers, “Effect of tilting on turbulent convection: Cylindrical samples with aspect ratio,” *J. Fluid Mech.* **715**, 314–334 (2013).
- <sup>40</sup>S.-X. Guo, S.-Q. Zhou, X.-R. Cen, L. Qu, Y.-Z. Lu, L. Sun, and X.-D. Shang, “The effect of cell tilting on turbulent thermal convection in a rectangular cell,” *J. Fluid Mech.* **762**, 273–287 (2015).
- <sup>41</sup>L. Zhang, G.-Y. Ding, and K.-Q. Xia, “On the effective horizontal buoyancy in turbulent thermal convection generated by cell tilting,” *J. Fluid Mech.* **914**, A15 (2021).
- <sup>42</sup>X.-Q. He, Y.-L. Xiong, A. D. Bragg, P. Fischer, and H. Kellay, “The effect of tilt on turbulent thermal convection for a heated soap bubble,” *Phys. Fluids* **34**, 105117 (2022).
- <sup>43</sup>Q. Wang, S.-N. Xia, B.-F. Wang, D.-J. Sun, Q. Zhou, and Z.-H. Wan, “Flow reversals in two-dimensional thermal convection in tilted cells,” *J. Fluid Mech.* **849**, 355–372 (2018).
- <sup>44</sup>S.-X. Guo, S.-Q. Zhou, L. Qu, X.-R. Cen, and Y.-Z. Lu, “Evolution and statistics of thermal plumes in tilted turbulent convection,” *Int. J. Heat Mass Transfer* **111**, 933–942 (2017).
- <sup>45</sup>G. Ahlers, E. Brown, and A. Nikolaenko, “The search for slow transients, and the effect of imperfect vertical alignment, in turbulent Rayleigh-Bénard convection,” *J. Fluid Mech.* **557**, 347 (2006).
- <sup>46</sup>D.-D. Ji, K.-L. Bai, and E. Brown, “Effects of tilt on the orientation dynamics of the large-scale circulation in turbulent Rayleigh-Bénard convection,” *Phys. Fluids* **32**, 075118 (2020).
- <sup>47</sup>P. Wei and K.-Q. Xia, “Viscous boundary layer properties in turbulent thermal convection in a cylindrical cell: The effect of cell tilting,” *J. Fluid Mech.* **720**, 140–168 (2013).
- <sup>48</sup>F. Chillá, M. Rastello, S. Chaumat, and B. Castaing, “Long relaxation times and tilt sensitivity in Rayleigh-Bénard turbulence,” *Eur. Phys. J. B* **40**, 223–227 (2004).
- <sup>49</sup>O. Shishkina and S. Horn, “Thermal convection in inclined cylindrical containers,” *J. Fluid Mech.* **790**, R3 (2016).
- <sup>50</sup>H.-D. Xi and K.-Q. Xia, “Flow mode transitions in turbulent thermal convection,” *Phys. Fluids* **20**, 055104 (2008).
- <sup>51</sup>H.-D. Xi, Y.-B. Zhang, J.-T. Hao, and K.-Q. Xia, “Higher-order flow modes in turbulent Rayleigh-Bénard convection,” *J. Fluid Mech.* **805**, 31–51 (2016).
- <sup>52</sup>H.-D. Xi, S. Lam, and K.-Q. Xia, “From laminar plumes to organized flows: The onset of large-scale circulation in turbulent thermal convection,” *J. Fluid Mech.* **503**, 47–56 (2004).
- <sup>53</sup>S.-Q. Zhou, Y.-C. Xie, C. Sun, and K.-Q. Xia, “Statistical characterization of thermal plumes in turbulent thermal convection,” *Phys. Rev. Fluids* **1**, 054301 (2016).